Electronic Journal of Applied Statistical Analysis
EJASA, Electron. J. App. Stat. Anal.
http://siba-ese.unisalento.it/index.php/ejasa/index
e-ISSN: 2070-5948
DOI: 10.1285/i20705948v11n1p269

Long-term constant acceleration can be sustained freely in running via stochastic short-term corrections

By Billat et al.

Published: 26 April 2018

Electronic Journal of Applied Statistical Analysis
Vol. 11, Issue 01, April 2018, 269-295
DOI: 10.1285/i20705948v11n1p269

Long-term constant acceleration can be sustained freely in running via stochastic short-term corrections

Véronique L. Billat[a], Jean-Pierre Koralsztein[b], Sophie Jacquot[c], and Nicolas J-B. Brunel*[d]

[a]*Laboratoire UBIAE, UEVE, University Paris Saclay, Evry, France*
[b]*Sports Medicine Center CCAS,Paris, France*
[c] *Laboratoire MAPMO, University of Orléans, Orléans, France*
[d] *LaMME, ENSIIE, University Paris Saclay, Evry, France*

Published: 26 April 2018

In the same way that most of the robots and advanced mobile machines are designed to optimize their energy consumption or the smoothness of their motions, it has been demonstrated that competitive runners tend to exhibit smoother strides than recreational runners during running and fast walking. Here, we describe the statistical mechanics of Humans trying to self-pace a constant acceleration, by studying the statistical properties of the accelerations of the runner's center of mass. Furthermore, it has been checked that this could be even achieved in a state of fatigue during exhaustive 3 self-pace ramp runs. For that purpose, we analyse a small sample of 3 male and 2 female middle-aged, recreational runners ran, in random order, three exhaustive self-paced acceleration trials (SAT) perceived to be "soft", "medium" or "hard". A statistical analysis shows that Humans can be able to self-pace constant acceleration in some exhaustive runs, by continuously adjusting the instantaneous accelerations. The variations of accelerations around the mean are ARMA stationary processes, which are similar, whichever acceleration levels and runners. The range of constant acceleration is very similar between runners and within the acceleration level. This work is the first step for understanding the Human optimisation of self-pace processes in exhaustive tasks such as running until exhaustion.

*Corresponding author: nicolas.brunel@ensiie.fr

ISSN: 2070-5948
http://siba-ese.unisalento.it/index.php/ejasa/index

keywords: pace, stochastic processes, stationarity, maximum likelihood estimation, ARIMA, running.

1 Introduction

Endurance running is considered to have played a key role in human evolution and Humans have developed the ability to fine-tune their running speed variations to run for several days and still catch their fastest prey (Bramble and Lieberman, 2004). Indeed, it has been reported that speed variation is the optimal way to optimise pace and achieving a given distance in a minimal time (Foster et al., 1993, 1994, 2004; Billat et al., 2001; Crouter et al., 2001; Sandals et al., 2006; Tucker et al., 2006; Tucker and Noakes, 2009).

However, there is a direct relationship between force impulse, running acceleration (Hunter et al., 2005) and the minimum-jerk model (Flash and Hogan, 1985) that predicts that running must be as smooth as possible and variations in acceleration must be close to 0 $m.s^{-3}$ in order to save energy and optimize performance. It has been demonstrated that competitive runners tend to exhibit smoother strides than recreational runners during both running and fast walking (Hreljac, 2000; Hreljac and Martin, 1993). Given that, it has been experimentally reported that speed variation is the optimal way of achieving the best running performance i.e. a given distance in a minimal time.

Our claim is that speed variations seems to be a general strategy chosen by runners for reaching specific race objectives, even simple "tasks" such as running at a constant acceleration. In this paper, we test the hypothesis that recreational runners are able to self-pace the acceleration of their center of mass in order to realise a constant acceleration race pattern globally. Furthermore, it has been checked that this could be even achieved in a state of fatigue during exhaustive 3 self-pace ramp runs.

Therefore, the present study tests the hypothesis whereby a small group of Humans can maintain a constant acceleration in a self-paced trial, regardless of the magnitude of acceleration and that this global constant acceleration is composed by stochastic accelerations that follow a stationary pattern until exhaustion.

2 Materials and Methods

We describe the exercise protocols and experimental data used in our study.

2.1 Subjects

The study population comprised three male and two female recreational runners (age 38 ± 3 yrs., total running distance per week: 36.1 ± 4.3 km; body weight: 66.9 ± 12.4 kg and height 171.1 ± 6.7 cm). All subjects were first informed of the risks and constraints associated with the protocol and gave their written, informed consent to participation. The present study conformed to the precepts of the Declaration of Helsinki and all procedures were approved by the local investigational review board (Saint Louis Hospital, Paris, France).

2.2 Experimental design

Subjects ran alone and performed four exhaustive runs (track tests) until exhaustion with a one-week interval between sessions: (i) the first track test was the Université de Montréal Track Test (Uger and Boucher, 1980) to estimate the velocity associated with peak oxygen uptake (vVO2max) (Billat and Koralsztein, 1996), (ii) the second, third and fourth track tests were self-paced acceleration trials (SATs) at respectively soft, medium and hard accelerations (in random order).

2.3 Exercise tests

2.3.1 The Université de Montréal Track Test

The Université de Montréal Track Test is a simple, indirect, continuous, multistage running field test for determining vVO2max (Berthoin et al., 1999). The subjects first ran for 2 minutes at 8 $km.h^{-1}$ and speed was increased by $1km.h^{-1}$ increments every 2 minutes until exhaustion. The velocity corresponding to the last, fully completed stage was recorded as the vVO2max.

2.3.2 Acceleration trials

In the Self-pace Acceleration Trials (SAT), the runners also started at a speed of 8 $km.h^{-1}$ and then increased their velocity at three different, constant accelerations (in random order). There was a two-hours interval between acceleration trials. The runners performed three freely paced acceleration sets in which they were asked to maintain constant acceleration by progressively increasing their speed until exhaustion, validated by the attainment of their maximal heart rate. The trials were run at three constant acceleration values, based on ratings of perceived acceleration ("soft", "medium" and "hard"). In the SAT set, no external information was provided to the runnner, except the distance covered. All tests were performed between 2 pm and 6 pm on wind-free, spring days ($< 2m.s^{-1}$ according to the Windwatch anemometer from ALBA, Silva, Sweden) with a temperature of 20°C, as in a previous study of the energetics of middle-distance running (Billat et al., 2004).

2.4 Data collected

Speed and acceleration were measured by the GPS-enabled Minimax accelerometer from Catapult Sports (Pty Ltd, Victoria, Australia). The difference between the true (track) and recorded (GPS) distance was less than 1% and 0.92% over 800 m and 1500 m, respectively. The heart rate was measured beat by beat with a Polar V800 monitor (Polar Electro Oy, Kempele, Finland). This result agrees with previous GPS studies for maximal efforts run by Humans or horses (Larsson, 2003; Larsson and Henriksson-Larsén, 2005). The limit time at the maximum heart rate i.e. the time to the plateau at the maximal heart rate was significantly different between the low and high acceleration ($p = 0.004$). The percentage of heart rate reserve which is known to be in accordance with the % of VO2max of the acceleration catch-up (Poole et al., 2008) (which was at

	Soft			*Medium*			*Hard*		
Subject	min	max	tlim	min	max	tlim	min	max	tlim
1	126	182	97	102	175	22	118	179	46
2	114	175	10	110	175	10	92	171	10
3	99	175	5	117	180	26	100	175	10
4	119	199	5	105	199	10	138	199	5
5	107	199	10	112	192	0	109	186	0
Mean	113	186	25.4	109.2	184.2	13.6	111.4	182	14.2
SD	10.4	12.2	40.1	5.9	10.8	10.4	17.8	11	18.2

Table 1: The minimal and maximal values of Heart Rate (in bpm) and delay of exhaustion (in seconds) at the maximal Heart Rate, denoted tlim, in SAT.

58 ± 14% vs. 72± 9% of time limit, $p = 0.04$) was not significantly different at this time (84 ± 7% vs. 79± 7% of time limit, $p = 0.15$).

The speed and acceleration of the center of mass are denoted respectively $(V_t)_{0\leq t\leq T}$ and $(A_t)_{0\leq t\leq T}$ where T is the total duration of each self-pace trial. When it is needed, we denote $V_t^{i,j}$, $A_t^{i,j}$ and $T_t^{i,j}$ the corresponding signals at time t, for individual $i = 1, \ldots 5$ and pace $j = S, M, H$ (for *Soft*, *Medium* and *Hard* pace respectively). We use a constant sampling time δ, and the objective is to characterise the mathematical properties of the acceleration signal $(A_t)_{t\geq 0}$ and of the associated discrete-time dynamical system

$$\begin{cases} V_{t+\delta} = & V_t + \delta A_t \\ D_{t+\delta} = & D_t + \delta V_t \end{cases} \tag{1}$$

where D_t is the distance ran at time t, starting at $D_0 = 0$. The constants $V_0 > 0$ and $A_0 > 0$ are respectively the initial speed and initial acceleration at the beginning of the trial (as indicated above, the trial started at a speed around 8 $km.h^{-1}$). We consider in the rest of the paper a sampling time $\delta = 1$ second. The GPS and accelerometer signals are respectively sampled at 5 Hz and 50 Hz and are finally averaged per second: our data, denoted $\hat{V}_t$ and $\hat{A}_t$ have a $1\,Hz$ frequency and are, respectively, direct estimates of the signals V_t and A_t appearing in our discrete time model (1).

Because of the measurement process and data averaging, the relationship $V_{t+1} = V_t + \delta A_t$ is not exactly satisfied by the empirical estimates $\hat{V}_t$ and $\hat{A}_t$. Nevertheless, the computed acceleration $\hat{\hat{A}}_t \triangleq \frac{\hat{V}_{t+1} - \hat{V}_t}{\delta}$ is highly correlated to the measured accelerations $\hat{A}_t$, as shown in table 2, see also figure 1. Conversely, the measured speed $\hat{V}_t$ and the integrated acceleration $\tilde{V}_t \triangleq \hat{V}_0 + \delta \sum_{i=1}^{t} \hat{A}_i$ are very highly correlated (between 0.97 and 0.99 for all the runners and intensities). In our analysis, the run distance at time t is directly computed from the measured speed with the relationship $\hat{D}_t = \hat{D}_{t-1} + \delta \hat{V}_t$ for $t \geq 1$ and $\hat{D}_0 = 0$.

	$Soft$	$Medium$	$Hard$
1	0.70	0.65	0.74
2	0.64	0.63	0.64
3	0.70	0.72	0.84
4	0.69	0.71	0.66
5	0.73	0.78	0.72

Table 2: Correlations between $(\hat{A}_t)$ and $(\hat{\hat{A}}_t)$ processes for the 5 runners and 3 intensities. All the p-values are $< 10^{-10}$.

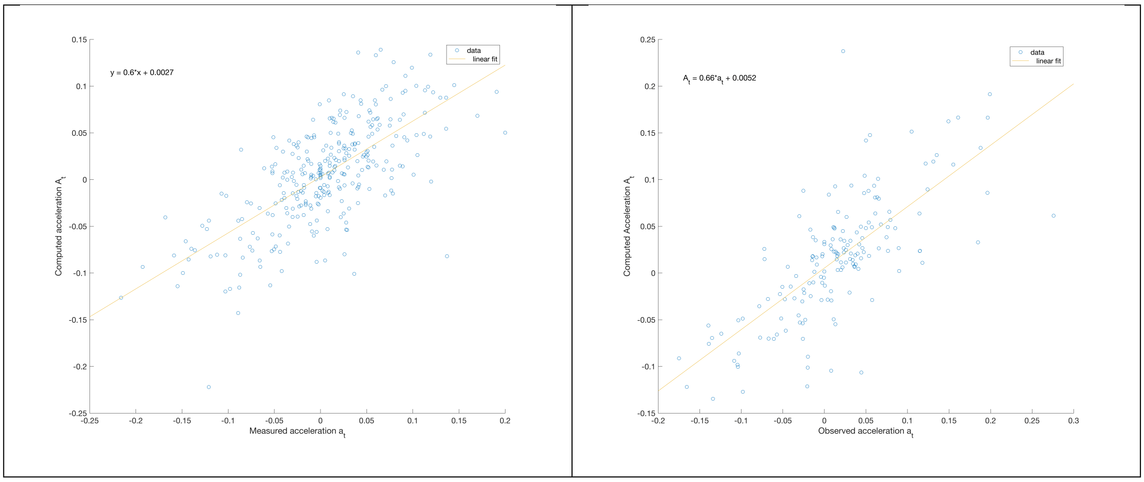

Figure 1: Plot of computed accelerations $(\hat{\hat{A}}_t)$ in $m.s^{-2}$ versus measured accelerations $(\hat{A}_t)$ $m.s^{-2}$ for runner 2, intensity *Medium* (Left) and for runner 5, intensity *Hard* (Right).

Soft	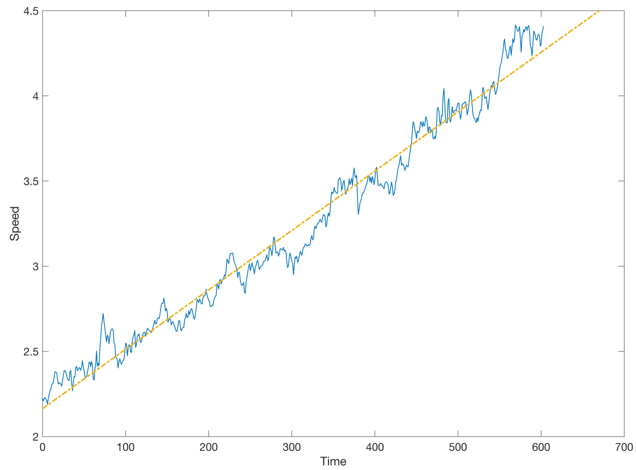
Medium	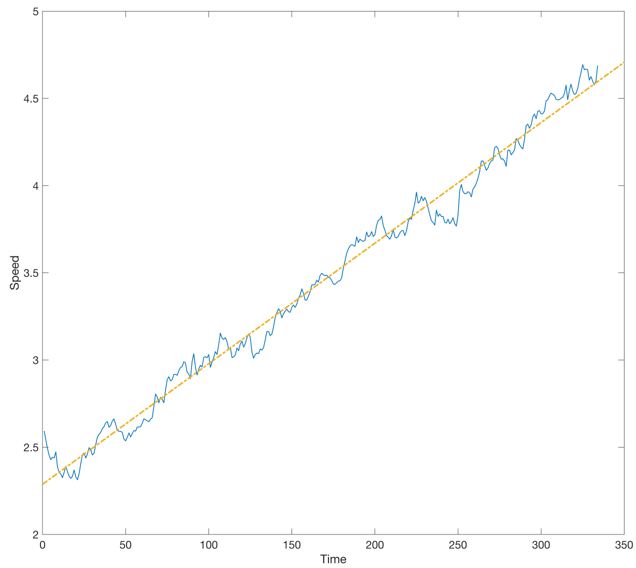
Hard	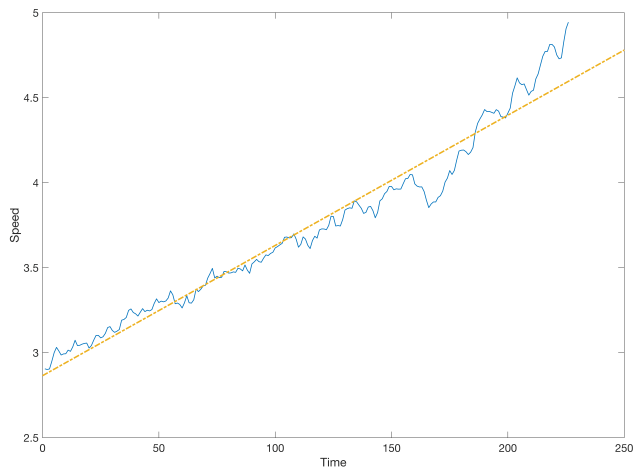

Figure 2: Measured speeds $\hat{V}_t$ $(m.s^{-1})$ versus Time (s) for Runner 4, with OLS linear trends (dashed lines): $\hat{V}_t^{4,S} = 0.0035t + 2.2$, $\hat{V}_t^{4,M} = 0.0069t + 2.3$, $\hat{V}_t^{4,H} = 0.0077t + 2.9$.

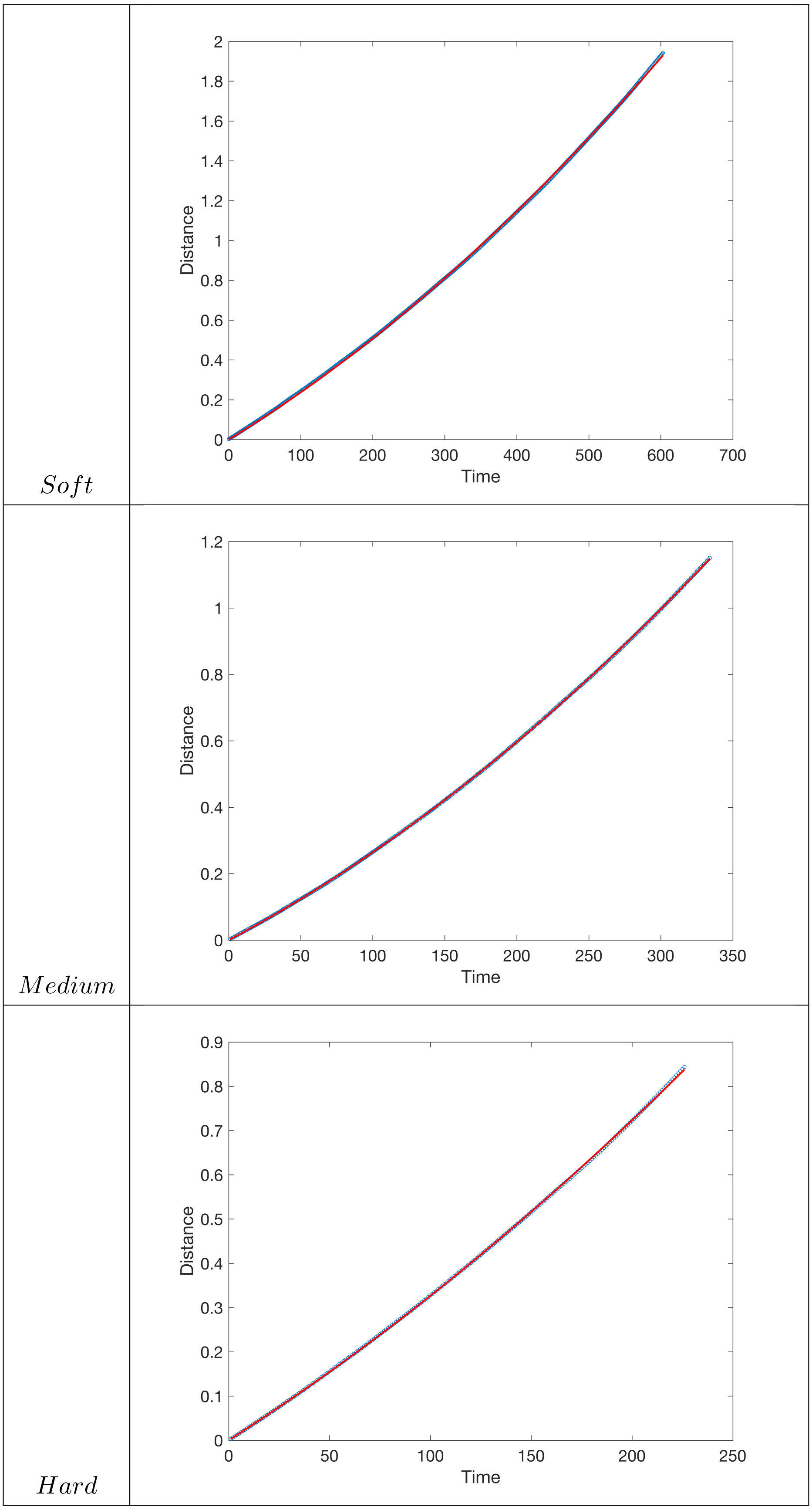

Figure 3: Distance (in km) versus Time (t in s) for Runner 4. Blue points: Computed Distance $\hat{D}_t$. Red Line : Quadratic Fit $\hat{D}_t = \mathbf{V}^{ols,d}t + \mathbf{A}^{ols,d}\frac{t(t+1)}{2}$.

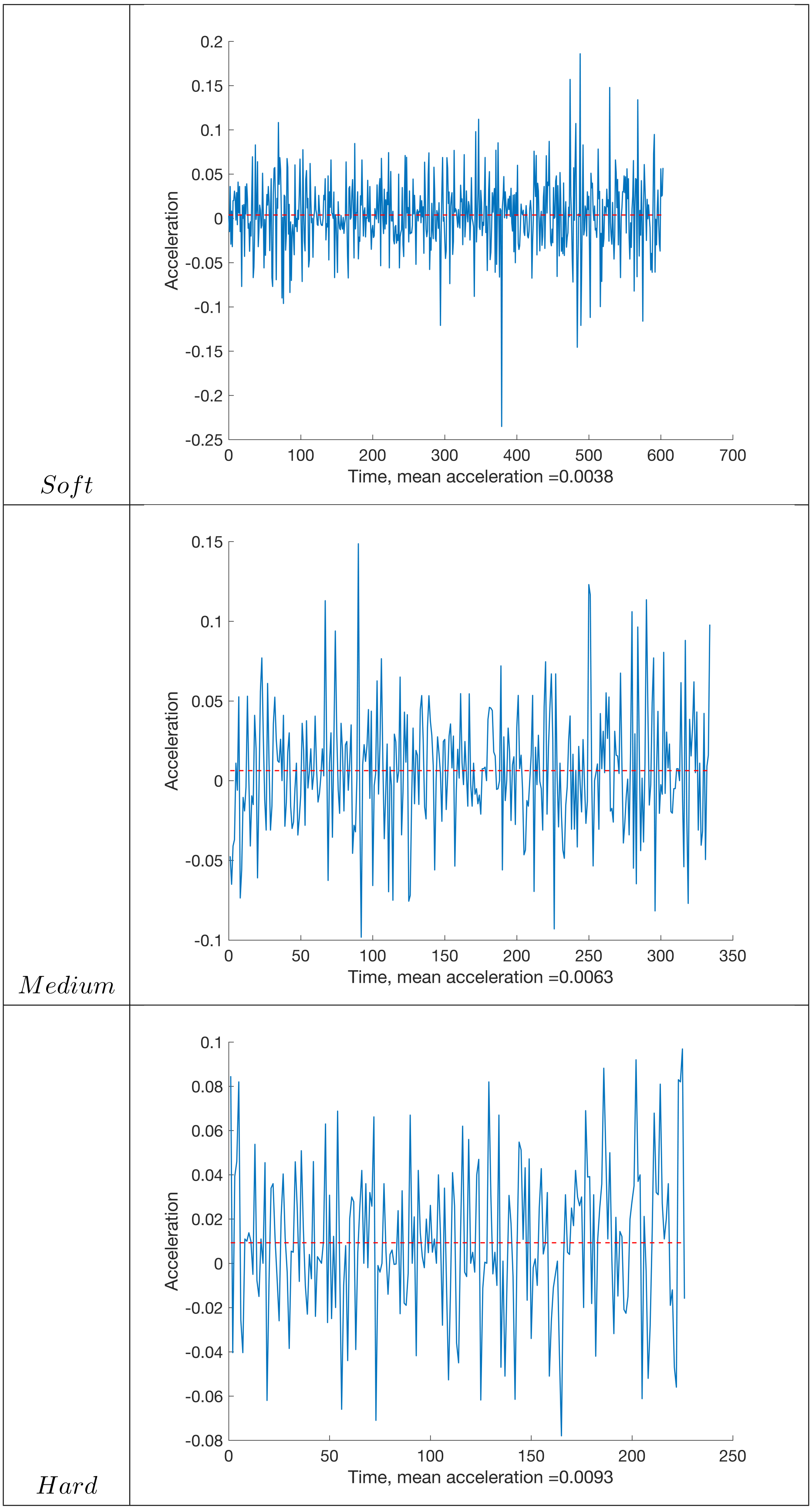

Figure 4: Acceleration $(\hat{A}_t)_{t\geq 0}$ versus Time (t in second) for Runner 4. Blue line: Measured acceleration, Red dashed Line: mean acceleration (in $m.s^{-2}$).

We now discuss the main patterns of the data $\left(\hat{V}_t\right)_{t\geq 0}$ that strongly support the fact that Humans can be able to freely sustain a constant acceleration. The plots of $(\hat{V}_t)_{t\geq 0}$ and $(\hat{D}_t)_{t\geq 0}$ are shown in figures 2 and 3 respectively. Under the assumption of a constant acceleration $\boldsymbol{A}$, the theoretical speed V_t and distance D_t satisfy respectively the linear and quadratic equations $V_t = V_0 + \boldsymbol{A}t$ and $D_t = V_0 t + \boldsymbol{A}\frac{t(t+1)}{2}$. Consequently, a linear trend fitting with Ordinary Least Squares (OLS) of the observed speed data $(\hat{V}_t)$ should reveal this remarkable pattern and give estimates of the initial speed and acceleration $\left(\hat{V}_0^{ols,v}, \hat{\boldsymbol{A}}^{ols,v}\right)$ by solving

$$\min_{V_0,A} \sum_{t=0}^{T} \left(\hat{V}_t - V_0 - At\right)^2.$$

In the same way, the distance data $\hat{D}_t$ can be fitted to a quadratic trend by solving

$$\min_{V_0,A} \sum_{t=0}^{T} \left(\hat{D}_t - V_0 t - A\frac{t(t+1)}{2}\right)^2$$

so that we can obtain alternative estimates $\left(\hat{V}_0^{ols,d}, \hat{\boldsymbol{A}}^{ols,d}\right)$.

While the speed seems to fluctuate randomly and significantly around the linear trend, we can consider that the estimated trend is globally correct, but stochastic variations are noticeable during the trial. Quite surprisingly, the quadratic trend for the run distance $\hat{D}_t$ fits almost perfectly the data (indeed R^2 is between 0.98 and 1).

The corresponding estimates $\hat{\boldsymbol{A}}^{ols,v}, \hat{\boldsymbol{A}}^{ols,d}$ are reported in table 3. The estimates can differ from each other; the main differences come from the variability of the measured initial speed $\hat{V}_0$ (see Figure 2) that perturb the simultaneous optimization in V_0 and A, while $\hat{D}_0$ is always set to 0. Nevertheless, they both provide coherent estimates of the long-term constant deterministic acceleration $\boldsymbol{A}^{i,j}$.

Finally, a third way of determining the constant acceleration $\boldsymbol{A}^{i,j}$ is the mean of the observed accelerations $\bar{\hat{\boldsymbol{A}}} = \frac{1}{T}\sum_{t=1}^{T}\hat{A}_t$, computed in table 4. The estimates $\hat{\boldsymbol{A}}^{ols,d}$ and $\bar{\hat{\boldsymbol{A}}}$ can be different as the distance data are much more smoother than the rough acceleration signal.

The remarkable perfect quadratic relationship between distance and time shows that the random variations observed in the speed $(\hat{V}_t)_{t\geq 0}$ does not accumulate across time; in fact, these variations seem to compensate each other, so that the distance run $\hat{D}_t$ becomes a deterministic quadratic function of time. A rapid analysis of the linear fit for the speed shows that the residuals $\hat{V}_t - V_0 - At$ are correlated, meaning that the basic linear model assumptions are not satisfied: the Durbin-Watson test reject the absence of autocorrelation of the residuals for all the trials. This suggests that there is a structure (and information) in the speed variations (and divergence from the linear trend). In the next section, we derive a proper setting for analysing the variations of the speed. In order to do that, we identify the stochastic structure of the acceleration processes A_t and the one of V_t by integration.

$\hat{\boldsymbol{A}}^{ols,v}/\hat{\boldsymbol{A}}^{ols,d}$ *in* $(m.s^{-2})$	*Soft*	*Medium*	*Hard*
1	0.0028/0.0029	0.0034/0.0039	0.0036/0.0040
2	0.0034/0.0032	0.0058/0.0051	0.016/0.0119
3	0.0036/0.0030	0.01/0.0086	0.019/0.0188
4	0.0035/0.0033	0.0069/0.0068	0.0077/0.0070
5	0.0017/0.0015	0.0041/0.0035	0.012/0.0128

Table 3: Estimates $\hat{A}^{ols,d}$ of mean acceleration $\boldsymbol{A}$ from the quadratic fit "Distance-Time" with Ordinary Least Squares ($\hat{D}_t = \hat{V}_0 t + \hat{A}^{ols,d}\frac{t(t+1)}{2} + e_t$).

$\bar{\hat{A}}$ $(m.s^{-2})$	*Soft*	*Medium*	*Hard*
1	0.0033	0.0053	0.0076
2	0.0054	0.0045	0.0193
3	0.0046	0.0107	0.0541
4	0.0038	0.0063	0.0093
5	0.0030	0.0050	0.0158

Table 4: Mean accelerations $\bar{\hat{\boldsymbol{A}}}^{i,j}$ computed from the measured accelerations ($\hat{A}_t^{i,j} \geq 0$).

2.5 Stochastic models

Our analysis of the speed and acceleration signals collected during the self-paced protocols shows that the speed $(\hat{V}_t)_{t\geq 0}$ and $(\hat{A}_t)_{t\geq 0}$ are realizations of stochastic processes that varies significantly during the Self-Pace Acceleration Trials, as shown in the previous section. For this reason, we introduce a stochastic model for describing the dynamics of $(V_t)_{t\geq 0}$ and $(A_t)_{t\geq 0}$. Indeed, if a runner i runs at a constant acceleration $\mathbf{A}$ during trial j, then we have for all $t = 1, 2, 3, \ldots$

$$\begin{cases} A_t^{i,j} = & \mathbf{A}^{i,j} \\ V_t^{i,j} = & V_0^{i,j} + \mathbf{A}^{i,j} t \\ D_t^{i,j} = & V_0^{i,j} t + \mathbf{A}^{i,j}\frac{t(t+1)}{2} \end{cases} \tag{2}$$

As seen in the previous section, this deterministic relationship is nearly satisfied for the distance $\hat{D}_t$, while there are significant deviation of $\hat{V}_t$ from a linear trend. In this section, we consider a general stochastic dynamical model with the same structure for all runners and intensities. For this reason, we remove the dependency on i and j.

2.5.1 A stochastic stationary acceleration model

A possible starting point for modelling the acceleration $(A_t)_{t\geq 0}$ is Newton's law, stating that for all $t = 1, 2, \ldots,$ the acceleration A_t is the sum of the forces applied to the center of mass of the runner. A well-studied family of such mechanistic models are bouncing ball models, where the human gait is decomposed in a series of "flight" and "contact" periods where leg stiffness, cadence,... play a prominent role, (see Blickhan, 1989; McMahon and Cheng, 1990; Farley et al., 1991; Bencsik and Zelei, 2017). From kinematics, it is possible to derive continuous time speed profiles, but such mechanistic models remain complex to analyze and depend on numerous assumptions about body's movement and phenomenological parameters that are individual dependent, and difficult to get. Additionally, the available data are sampled and then averaged, such that such continuous time and detailed models might be hard to assess experimentally.

We use a coarser-grain stochastic model: we assume that a runner cannot maintain a constant deterministic acceleration $\mathbf{A}$, but he/she is able to realize a stochastic acceleration that varies around a given mean $\mathbf{A}$ (at each time t), as it is suggested by the plots of $\left(\hat{A}_t\right)_{t\geq 0}$ in figure 4. This is our first assumption.

Claim 1. *Let (Z_t) be the process of variations around the mean such that $A_t = \mathbf{A} + Z_t$, where by definition the expectations $E[Z_t] = 0$ for all $t \geq 0$. Our model describes the acceleration of the center of gravity of the runner, its speed and run distance by the stochastic model*

$$\begin{cases} A_t = & \mathbf{A} + Z_t \\ V_t = & V_0 + \mathbf{A}t + Y_t \\ D_t = & V_0 t + \mathbf{A}\frac{t(t+1)}{2} + X_t \end{cases} \tag{3}$$

for $t \geq 1$, with $Y_0 = X_0 = 0$. A_0, V_0 are the initial (random) acceleration and speed at the beginning of a trial. $\triangle$

The processes $(Z_t)_{t\geq 0}$, $(Y_t)_{t\geq 0}$ and $(X_t)_{t\geq 0}$ are the discrepancies between the deterministic constant acceleration pattern (2) and the true observed processes. Because of the relationship (1), these 3 processes are related such that

$$\begin{cases} Y_t = & Y_{t-1} + Z_t \\ X_t = & X_{t-1} + Y_t \end{cases}$$

This means that $Y_t = \sum_{i=1}^{t} Z_i$ and $X_t = \sum_{i=1}^{t} (t+1-i) Z_i$ (we recall that the time lag is $\delta = 1s$). Our model helps to consider two accelerations: a long term acceleration $\mathbf{A}$ and a short-term acceleration $(A_t)_{t\geq 0}$. The long term acceleration can be tuned and maintained by a runner, but it is obtained by real-time and stochastic accelerations. Our model describes how the instantaneous variations Z_t helps in getting a long term pattern $V_0 + \mathbf{A}t$ for the speed, or the trend $V_0 t + \mathbf{A}\frac{t(t+1)}{2}$ for the distance.

We assume that $(Z_t)_{t\geq 0}$ is a weak stationary process with mean $E[Z_t] = 0$, variance $V(Z_t) = \sigma_Z^2 < \infty$ and a covariance function $cov(Z_t, Z_s) = E[Z_t Z_s] = \gamma(t-s)$ that is time-translation invariant, (see Hamilton, 1994). More precisely, our fundamental assumption is the following

Claim 2. *$(Z_t)_{t\geq 0}$ is an $ARMA(p,q)$ process (AutoRegressive and Moving Average): there exists two integers $p, q \geq 1$ and real parameters $\phi_1, \ldots, \phi_p$ and $\theta_1, \ldots, \theta_q$ such that*

Z_t satisfies the evolution equation

$$Z_t = \phi_1 Z_{t-1} + \cdots + \phi_p Z_{t-p} + e_t + \theta_1 e_{t-1} + \ldots \theta_q e_{t-q} \tag{4}$$

where $(e_t)_{t \geq 0}$ is a white noise process (i.e $V(e_t) = \sigma_e^2$, $cov(e_t, e_s) = 0$ if $t \neq s$), and is independent of the previous variations $Z_s, s < t$. We can write the corresponding model for the acceleration process $(A_t)_{t \geq 0}$ that satisfies the slightly modified evolution equation

$$A_t = \mathbf{f} + \phi_1 A_{t-1} + \cdots + \phi_p A_{t-p} + e_t + \theta_1 e_{t-1} + \ldots \theta_q e_{t-q}. \tag{5}$$

The constant $\mathbf{f}$ and the mean acceleration $\mathbf{A}$ are related by the following equation

$$\left(1 - \sum_{i=1}^{p} \phi_i\right) \mathbf{A} = \mathbf{f},$$

obtained by exploiting the fact that $E[A_t] = \mathbf{A}$, for all $t \geq 0$. $\triangle$

Equation (5) permits a mechanistic interpretation of our model in the spirit of Newton's law: the intercept $\mathbf{f}$ is the mean force applied to the center of gravity of the runner, while the AutoRegressive part $\phi_1 A_{t-1} + \cdots + \phi_p A_{t-p}$ accounts for the inertial effect of the body mass, p is the size of the memory. The Moving Average part $e_t + \theta_1 e_{t-1} + \ldots \theta_q e_{t-q}$ corresponds to the forces applied by the runner between times $t-1$ and t. If $\theta_1 = \cdots = \theta_q = 0$, this part reduces to e_t, that is independent from the previous accelerations A_t and of the previous forces $e_{t-1}, e_{t-2}, \ldots$. In some way, the variable e_t corresponds to the bouncing forces applied during the "contact period". This latter situation might be unrealistic, as the gait mouvement due to successive bounces might imply that the bouncing forces applied at each time t depends on the previous bounces. For this reason, the bouncing forces are modelled by a Moving Average $e_t + \theta_1 e_{t-1} + \ldots \theta_q e_{t-q}$ that can take into account the correlation between bouncing forces (q is the corresponding size of the memory in seconds). The parameters $\boldsymbol{\phi} = (\phi_i)_{1 \leq i \leq p}$ and $\boldsymbol{\theta} = (\theta_j)_{1 \leq j \leq q}$ are a condensed way of describing globally the dynamics of a runner (and somehow the gait, strength, stiffness, cadence,...) in a way that it can be easily estimated from the acceleration data $\hat{A}_t$, typically by Maximum Likelihood. These parameters are univoquely related to the autocovariance function of the process $\gamma_Z(h) = cov(Z_t, Z_{t-h}) = \gamma_Z(h; \boldsymbol{\theta}, \boldsymbol{\phi}, \sigma_Z^2)$, and control its shape and patterns (and of course the autocorrelation function $\rho_Z(h; \boldsymbol{\theta}, \boldsymbol{\phi}) \triangleq \frac{\gamma_Z(h; \boldsymbol{\theta}, \boldsymbol{\phi})}{\sigma_Z^2}$). An interesting feature, among others, is the geometric decay of the covariance, for h greater that q.

Finally, we assume that the process $(A_t)_{t \geq 0}$ is a Gaussian process, meaning that we assume that the random vector $\mathbf{Z} = (Z_1\, Z_2 \ldots Z_T)^\top$ in $\mathbb{R}^T$ is a Gaussian vector with zero mean and covariance matrix Γ_Z in $\mathbb{R}^{T \times T}$ with elements $\gamma_Z(i-j; \boldsymbol{\theta}, \boldsymbol{\phi}, \sigma_Z^2)$ for $1 \leq i, j \leq T$. For estimating the parameters, we use the Gaussian conditional log-likelihood of the data $\hat{A}_t$ (f is the joint density of the data):

$$\mathcal{L}\left(\hat{A}_1,\ldots,\hat{A}_T;\boldsymbol{\theta},\boldsymbol{\phi},\sigma_Z^2\right) = \log f\left(\hat{A}_1,\ldots,\hat{A}_T|\hat{A}_0\hat{A}_1,\ldots,\hat{A}_p;\boldsymbol{\theta},\boldsymbol{\phi},\sigma_Z^2\right) \tag{6}$$
$$= -\frac{T}{2}\log(2\pi) - \frac{T}{2}\log\sigma_Z^2 - \sum_{t=1}^{T}\frac{\hat{e}_t^2}{2\sigma_Z^2}$$

where $\hat{e}_t = \hat{A}_t - \boldsymbol{A} - \sum_{i=1}^{p}\phi_i\hat{A}_{t-i} - \sum_{j=1}^{q}\theta_j\hat{e}_{t-j}$ are the innovations, that are computed recursively for $t > q-1$.

2.5.2 Speed and Distance models: linear regression with correlated errors

Speed and distance are obtained by successive integrations as it is shown in equation (3). The deterministic part $V_0 + \mathbf{A}t$ is the "long-term" trend achieved by continuous variations of the speed Y_t, that are correlated as they depend on the current speed, and the previous corrections $Y_{t-1}, Y_{t-2}, \ldots$ The statistical model $V_t = V_0 + \mathbf{A}t + Y_t$ cannot be interpreted as a standard linear regression, as Y_t is not a white noise, i.e it does not satisfy the assumption $cov(Y_t, Y_s) \neq 0$. Indeed, the process $(Y_t)_{t\geq 0}$ is an integrated ARMA process (denoted ARIMA process, see Chapter 17 in (Hamilton, 1994)). This means that although $E[Y_t] = 0$ for all t, the covariances $E(Y_tY_{t-h})$ change with t.

A direct consequence of our acceleration model is that speed model is a linear regression with correlated errors $(Y_t)_{t\geq 0}$ that can be written in matrix form. We denote $\boldsymbol{V} = (V_t)_{t=1..T}$ in $\mathbb{R}^T$, $\boldsymbol{M} = \begin{bmatrix} 1 & 1 & \cdots & 1 \\ 1 & 2 & \cdots & T \end{bmatrix}^\top$ and $\boldsymbol{Y} = (Y_t)_{t=1..T}$. The linear regression model is

$$\boldsymbol{V} = \boldsymbol{M}\begin{pmatrix} V_0 \\ \mathbf{A} \end{pmatrix} + \boldsymbol{Y} \tag{7}$$

From our model assumptions, the vector $\boldsymbol{Y}$ satisfies $E[\boldsymbol{Y}] = 0$ and has a covariance matrix $\Sigma_Y(\boldsymbol{\theta},\boldsymbol{\phi},\sigma_Z^2) = cov(\boldsymbol{Y}) \in \mathbb{R}^{T\times T}$ that depends on the parameters of the process $(Z_t)_{t\geq 0}$, in particular the covariance matrix Σ_Y is not diagonal. The parameters $V_0, \mathbf{A}, \Sigma_Y$ can be estimated from the speed data $(\hat{V}_t)$ by Maximum Likelihood estimation, without the need to observe the process Y_t (nor Z_t).

In the same way, the distance model is a linear regression with ARIMA errors

$$\boldsymbol{D} = \boldsymbol{N}\begin{pmatrix} V_0 \\ \mathbf{A} \end{pmatrix} + \boldsymbol{X} \tag{8}$$

where $\boldsymbol{D} = (D_t)_{t=1..T}$ denotes the vector of run distances in $\mathbb{R}^T$,

$$\boldsymbol{N} = \begin{bmatrix} 1 & 2 & \cdots t \cdots & T \\ 1 & 3 & \cdots \frac{t(t+1)}{2} \cdots & \frac{T(T+1)}{2} \end{bmatrix}^\top$$

Runner / Intensities	S	M	H
1	$-10.79\,(<0.01)$	$-12.32\,(<0.01)$	$-10.61\,(<0.01)$
2	$-18.00\,(<0.01)$	$-13.78\,(<0.01)$	$-9.40\,(<0.01)$
3	$-11.47\,(<0.01)$	$-9.31\,(<0.01)$	$-9.31\,(<0.01)$
4	$-14.06\,(<0.01)$	$-15.41\,(<0.01)$	$-9.83\,(<0.01)$
5	$-18.29\,(<0.01)$	$-12.88\,(<0.01)$	$-7.30\,(<0.01)$

Table 5: Augmented Dickey-Fuller Test Statistics and p-value for stationarity of acceleration data ($\hat{A}_t^{i,j}$)

is the design matrix in $\mathbb{R}^{T\times 2}$ and $\boldsymbol{X} = (X_t)_{t=1..T}$ is the vector of correlated errors in $\mathbb{R}^T$.

3 Results

In this section, we present the statistical inference of our models from the available data $\left(\hat{A}_t^{i,j}\right)_{t=1...T}$ and $\left(\hat{V}_t^{i,j}\right)_{t=1...T}$ described in section 2.4. Our analysis is two-fold: we analyze in a first stage only the accceleration data, and we check that Claim 2 (assumption of a stationary ARMA model for acceleration) is correct in all cases. In a second stage, we analyze the speed data $\left(\hat{V}_t^{i,j}\right)_{t=1...T}$ based on the regression models discussed in section 2.5.2.

3.1 Acceleration data and models

3.1.1 Stationarity test

The first property to test from the data is the stationarity assumption. We use the Augmented Dickey-Fuller test (ADF test) in order to test the existence of a unit-root in the observed process $\left(\hat{A}_t\right)_{t=1...T}$ by estimating the model $A_t = \alpha + \varphi A_{t-1} + \delta_1 \Delta A_{t-1} + \cdots + \delta_p \Delta A_{t-p} + e_t$ based on an OLS regression (and test the assumption $\varphi = 1$). The results are given in table 5. For all trials, the null assumption $\varphi = 1$ (i.e unit root) is rejected: the standard ADF test is performed after selection of the best time lags p between 1 and 10 based on AIC.

The Unit-Root assumption for acceleration is strongly rejected (with p-value lower than 1.10^{-2}) for every trial. We have considered the existence of a constant α, as well as of a deterministic time trend $\alpha + \gamma t$ in the ADF test. In this latter situation, the Unit-Root assumption is also always rejected with a p-value lower than 1.10^{-2}.

3.1.2 Selection of p and q

The standard approach for the estimation of $ARMA(p, q)$ model consists in selecting first the autoregressive and moving average orders p and q respectively from the data,

BIC ($\times 10^3$) ; $\hat{p}$	S	M	H
1	-1.81 ; 2	-1.34 ; 2	-0.60 ; 2
2	-1.02 ; 2	-0.80 ; 2	-0.31 ; 2
3	-1.63; 2	-0.65; 2	-0.12; 3
4	-2.18; 1	-1.25; 3	-0.89; 1
5	-3.45; 2	-1.62; 2	-0.41; 2

Table 6: BIC criterion for the selection of $p \in [1 \dots 20]$ when $q = 1$

BIC ($\times 10^3$) ; $\hat{p}$	S	M	H
1	-1.82 ; 1	-1.35 ; 2	-0.60 ; 3
2	-1.02 ; 1	-0.80 ; 1	-0.31 ; 1
3	-1.63; 1	-0.65; 1	-0.12; 3
4	-2.18; 1	-1.25; 1	-0.89; 2
5	-3.45; 1	-1.62; 2	-0.41; 1

Table 7: BIC criterion for the selection of $p \in [1 \dots 20]$ when $q = 2$

and then to compute the parameters for the selected parameters $(\hat{p}, \hat{q})$. We estimate first the parameters $\boldsymbol{A}^{i,j}$ with the mean of the acceleration $\hat{A}_t^{i,j}$, and we use the estimated variations $\hat{Z}_t^{i,j} = \hat{A}_t^{i,j} - \boldsymbol{A}^{i,j}$. We have restricted the search to $q = 1, 2$ and $p = 1, \dots, 10$: we select p, q by minimizing the BIC defined as $BIC(p, q) = -2\mathcal{L}(\hat{\boldsymbol{\theta}}, \hat{\boldsymbol{\phi}}, \sigma_Z^2) - (p+q) \log T$ where $\mathcal{L}$ is the log-likehood of the $ARMA(p, q)$ model as defined in eq. (6). We give the values of the couple $(\hat{p}_1, BIC(\hat{p}, 1))$ in table 6 and $(\hat{p}_2, BIC(\hat{p}, 2))$ in table 7: The values of the BIC are similar in both cases for all trials. We choose finally the sparser model by selecting $\hat{q} = 1$ for all i, j. Indeed, the partial autocorrelograms in figure 5 suggest that the second partial correlation is significantly different from 0, while the first partial autocorrelation vanishes, which might suggest that $p = 2$ is more appropriate.

Finally, regarding the BIC values reported in table 6, the choice $(\hat{p}, \hat{q}) = (2, 1)$ seems more appropriate as the choice $\hat{p}_1 = 2$ is more stable across trials than the choice $\hat{p}_2$ in table 7. Anyway, it is clear from the fast decays in the autocorrelograms and partial autocorrelograms that the orders p, q should be quite small.

3.1.3 Parameter estimates and autocorrelations

We fit in this section an $ARMA(2, 1)$ to all the trials meaning that our model for acceleration is

$$A_t^{i,j} - \boldsymbol{A}^{i,j} = \phi_1 \left(A_{t-1}^{i,j} - \boldsymbol{A}^{i,j} \right) + \phi_2 \left(A_{t-2}^{i,j} - \boldsymbol{A}^{i,j} \right) + e_t + \theta_1 e_{t-1}$$

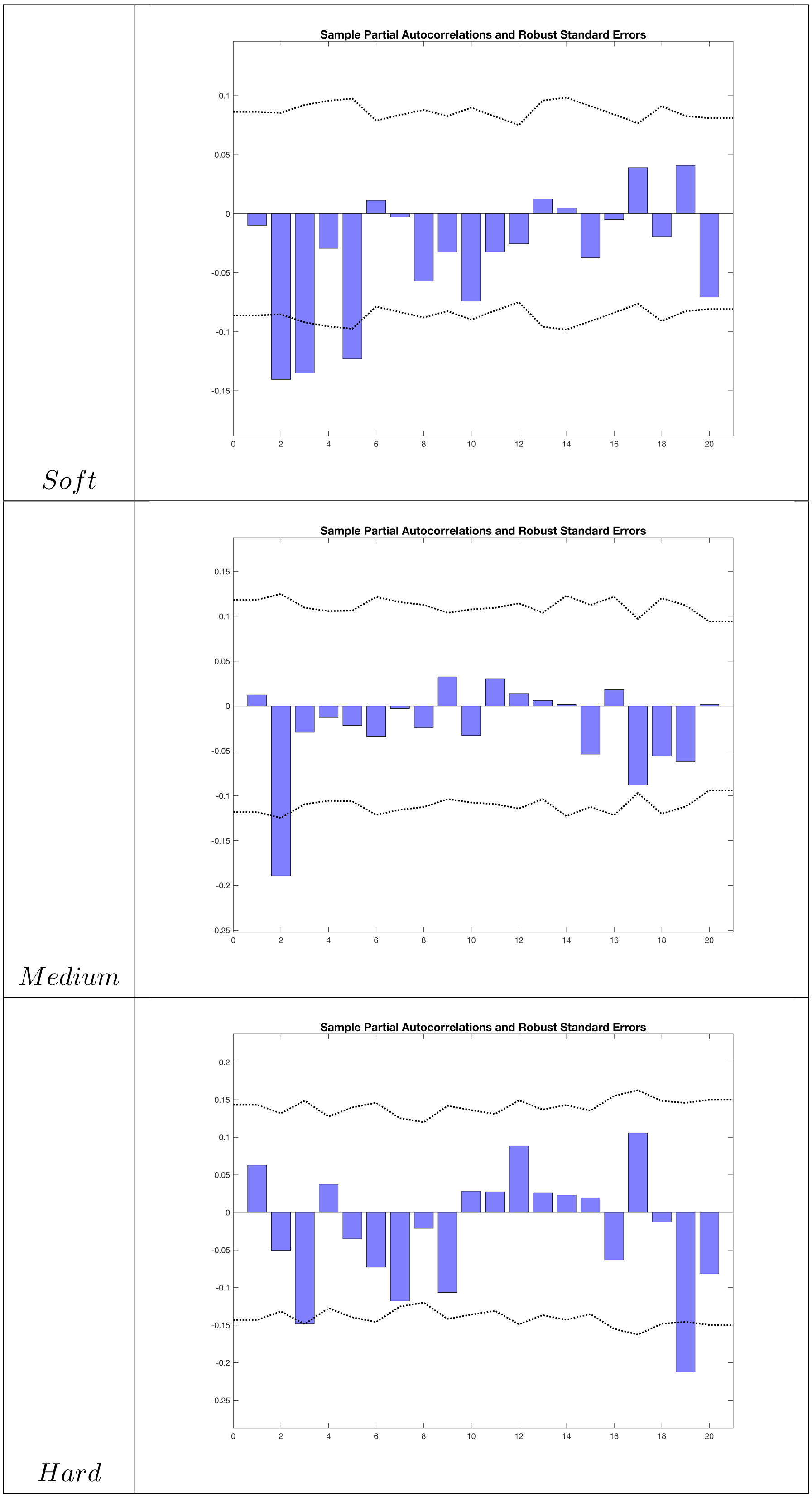

Figure 5: Partial Autocorrelations of the accelerations $(\hat{A}_t)$ for Lag $= 1, \ldots, 10\,seconds$, with robust confidence bands for Runner 4.

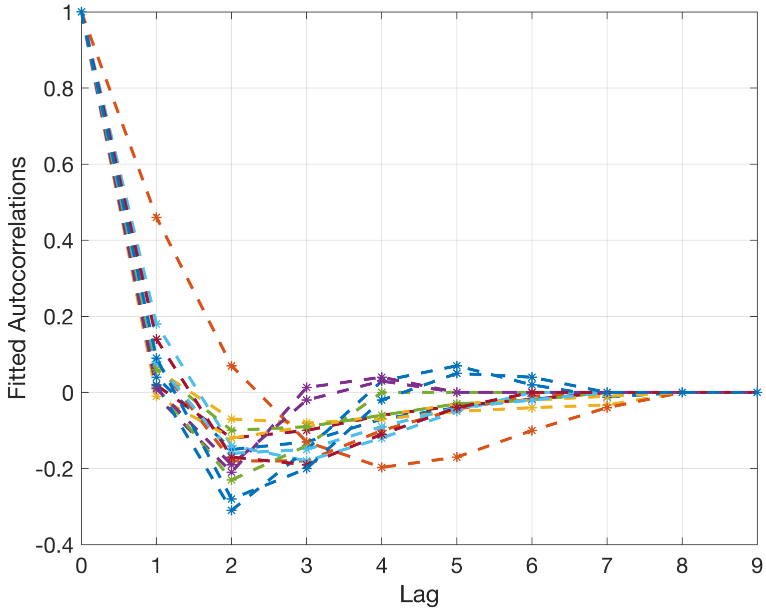

Figure 6: Partial Autocorrelations of the accelerations ($\hat{A}_t$) for Lag $= 0, \ldots, 9$ for all the runners and all intensities.

and $V(e_t) = \sigma^2_{i,j}$. The parameter estimates are obtained by maximum likelihood, and are collected in table 8. The estimates have a similar profile (mean parameters are $\bar{\phi}_1 = 0.70$, $\bar{\phi}_2 = -0.24$ and $\bar{\theta}_1 = -0.65$), that corresponds to empirical and fitted correlation functions $h \mapsto \rho\left(h, \hat{\boldsymbol{\phi}}^{i,j}\hat{\boldsymbol{\theta}}^{i,j}\right)$, as shown in figure 7. A remarkable feature of the estimated autocorrelation functions (and empirical counterparts) is that

$$\begin{cases} \rho\left(1, \hat{\boldsymbol{\phi}}^{i,j}, \hat{\boldsymbol{\theta}}^{i,j}\right) & \approx 0 \\ \rho\left(h, \hat{\boldsymbol{\phi}}^{i,j}, \hat{\boldsymbol{\theta}}^{i,j}\right) & \approx -0.2,\ h = 2, 3 \\ \rho\left(h, \hat{\boldsymbol{\phi}}^{i,j}, \hat{\boldsymbol{\theta}}^{i,j}\right) & \approx 0,\ h \geq 4 \end{cases}$$

for all i, j, as we can see in figure 6. Indeed, all the estimated autocorrelations have the same decreasing pattern with vanishing autocorrelation at lag $h = 1$, as described above. The estimated autocorrelations $\rho\left(1, \hat{\boldsymbol{\phi}}^{i,j}, \hat{\boldsymbol{\theta}}^{i,j}\right)$ are below the significance threshold (95% significance) in all cases, except for runner 3 at intensity *Hard*. Nevertheless, it should be noticed that the pattern is the same, but with a time shift between 1 and 2 seconds. If we remove this latter race, we find that the mean 1rst order autocorrelation accross intensities and runners is 0.055, with a standard deviation equals to 0.053. The mean autocorrelations of $\rho\left(2, \hat{\boldsymbol{\phi}}^{i,j}, \hat{\boldsymbol{\theta}}^{i,j}\right)$ and $\rho\left(3, \hat{\boldsymbol{\phi}}^{i,j}, \hat{\boldsymbol{\theta}}^{i,j}\right)$ are respectively -0.17 and -0.12 (with standard deviations equal to 0.6). For higher order autocorrelations ($h \geq 4$), the

Runner	Intensity	ϕ_1	ϕ_2	θ_1
1	S	0.82	−0.18	−0.82
	M	0.85	−0.26	−0.85
	H	0.96	−0.14	−0.92
2	S	−0.05	−0.21	0.04
	M	0.57	−0.24	−0.60
	H	0.89	−0.31	−0.71
3	S	0.79	−0.14	−0.80
	M	0.47	−0.33	−0.51
	H	1.20	−0.48	−0.69
4	S	0.80	−0.12	−0.85
	M	0.12	−0.20	−0.11
	H	0.82	−0.16	−0.76
5	S	0.86	−0.23	−0.84
	M	0.86	−0.30	−0.75
	H	0.61	−0.34	−0.57

Table 8: Acceleration data: parameters estimates for $ARMA(2,1)$

estimates are not significant.

This is a neat pattern shared by all runners for all trial intensities, that indicates a negative correlation in the accelerations between 2 and 3 seconds. At a larger time scale, the accelerations are uncorrelated. A surprising outcome, respected by the models is that the acceleration changes $A_t^{i,j} - \boldsymbol{A}^{i,j}$ are not correlated within a time period less than 2 seconds.

Finally, we have analysed the estimated residuals $\hat{e}_t^{i,j}$ of the ARMA model, in order to detect a possible lack-of-fit. The plots are given in the *Supplementary Information 1*, and reveal that any case, there is no information left in the correlation structure of the residuals: all the correlations and partial autocorrelations are not significantly different from 0. The QQ-plots show that in most of the trials, the acceleration can be considered Gaussian, except for runner 3 and the *Soft* trials for runners 2 and 5 where few important variations (negative or positive) are more observed with respect to the Gaussian case. Such heavier tails could be considered by using a Student distribution instead of a Gaussian distribution, but the covariance structure of the data is correctly reproduced in all the cases.

3.2 Models from speed data

We estimate the regression model $V_t = V_0 + \mathbf{A}t + Y_t$ from the speed data $\left(\hat{V}_t\right)_{t=1\ldots T}$. Following section 3 and statistical results of the previous section, we assume that the

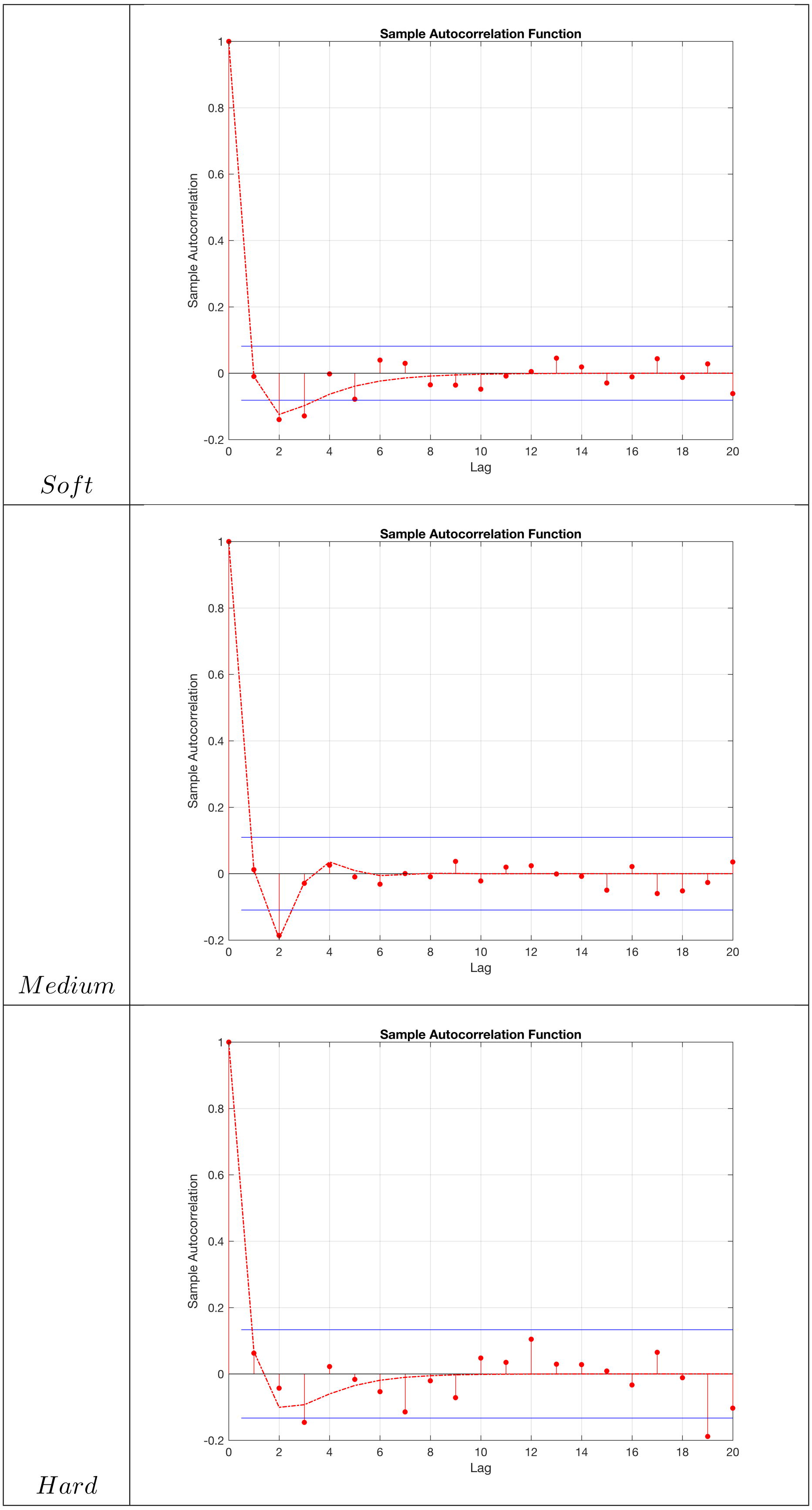

Figure 7: Autocorrelogram of the accelerations ($\hat{A}_t$) for Lag $= 1, \ldots, 10$ *seconds* for Runner 4. Horizontal blue lines are significance bands (correlations within these lines are not significantly different of 0 with a 5% risk). The dotted lines are estimated autocorrelograms $\rho\left(h, \hat{\boldsymbol{\theta}}, \hat{\boldsymbol{\phi}}\right)$ for the selected $ARMA(2,1)$ model.

Runner	Trial	$\mathbf{A}$ ($\times 10^{-3}$)	ϕ_1	ϕ_2	θ_1	σ_e	Q (p-value)
1	S	2.7 (1.5)	0.28 (0.17)	-0.31 (0.04)	-0.08 (0.18)	0.04	6.8 (0.34)
	M	4.2 (0.9)	0.82 (0.1)	-0.33 (0.05)	-0.75 (0.1)	0.04	15.1 (0.02)
	H	6.8 (3.7)	0.31 (0.17)	-0.31 (0.09)	0.10 (0.18)	0.05	2.6 (0.85)
2	S	3.5 (2.7)	0.05 (0.18)	-0.33 (0.05)	0.09 (0.2)	0.06	7.5 (0.27)
	M	6.5 (1.8)	0.61 (0.13)	-0.38 (0.05)	-0.51 (0.14)	0.05	14 (0.02)
	H	18.6 (5.9)	-0.15 (0.22)	-0.28 (0.09)	0.29 (0.22)	0.08	11.1 (0.08)
3	S	4.7 (1.9)	0.57 (0.25)	-0.3 (0.04)	-0.36 (0.26)	0.05	13.6 (0.03)
	M	10.7 (3.2)	0.21 (0.18)	-0.39 (0.06)	-0.02 (0.2)	0.06	8.5 (0.19)
	H	22.5 (12.9)	0.47 (0.26)	-0.41 (0.15)	0.19 (0.30)	0.10	4.6 (0.58)
4	S	3.6 (1.1)	0.56 (0.19)	-0.31 (0.04)	-0.37 (0.21)	0.03	10.7 (0.10)
	M	6.3 (1.6)	0.27 (0.34)	-0.21 (0.07)	-0.10 (0.35)	0.03	1.84 (0.93)
	H	8.8 (1.5)	1.01 (0.18)	-0.33 (0.06)	-0.71 (0.18)	0.02	2.8 (0.83)
5	S	2.7 (0.8)	0.98 (0.05)	-0.4 (0.03)	-0.75 (0.05)	0.05	32.2 (10^{-5})
	M	4.6 (2.4)	0.11 (0.22)	-0.25 (0.09)	0.29 (0.23)	0.05	26.5 (10^{-4})
	H	15.5 (3.4)	0.57 (0.23)	-0.40 (0.07)	-0.40 (0.26)	0.06	4.9 (0.54)

Table 9: Estimated Parameters for Speed Regression with ARIMA errors

errors Y_t are correlated, with $ARIMA(2,1,1)$ structure. The estimation procedure uses the differenced data $\hat{\hat{A}}_t = \hat{V}_t - \hat{V}_{t-1}$ and the fact that

$$V_t - V_{t-1} = \mathbf{A} + (Y_t - Y_{t-1})$$

is an $ARMA(2,1)$ process with a constant, as $Y_t - Y_{t-1} = Z_t$. The estimates are provided in table 9 and give a correct fit to the data. Indeed, we compute the Q statistics of the Ljung-Box test for the presence of autocorrelations in the residuals. We accept the assumption of "uncorrelation" of the residuals in 10 trials out of 15, which means that the estimated $ARIMA(2,1)$ takes into account the correlation structure of the speed data $\hat{V}_t$. The 5 cases having a p-value lower than 5% corresponds to cases where 1 or 2 autocorrelations $|\rho(h)|$ for $h > 2$ are between 0.1 and 0.2. In these latter case, we can estimate $ARIMA(p,1,q)$ models with p,q adaptively selected (but lower than 3), that gives uncorrelated residuals with Ljung-Box test.

4 Discussion

To the best of our knowledge, a human's ability to maintain constant acceleration in a conscious way until exhaustion has not yet been investigated, and in no case with a statistical approach. We therefore decided to test the hypothesis whereby humans are able to maintain a constant acceleration, regardless of the speed and the magnitude of acceleration. Despite the large published body of work on pacing strategy and speed control (especially concerning feedback vs. feed forward power output control and central vs. peripheral mechanisms, (Ariyoshi et al., 1979; Zamparo et al., 2001; Lambert et al., 2004; Abbiss and Laursen, 2008; De Koning et al., 2011; Ansley et al., 2004), this is the first study to have examined acceleration control during running. Our results show that runners are able to control their acceleration until exhaustion at three significantly different accelerations values perceived to be "soft, medium and hard". We determined that humans can precisely regulate their acceleration (regardless of its intensity) in a run leading to exhaustion in 3 to 14 minutes. Indeed, our data showed that runners can (i) apply distinct, subjective acceleration values when so instructed, (ii) maintain constant acceleration until exhaustion, regardless of the acceleration value and that the maximal heart rates plateau for each different level of perceived acceleration (soft, medium, hard). The range of these perceived acceleration values is in accordance with accelerations measured in correspondance to those observed in middle-distance running (Billat et al., 2009).

We support these claims thanks to the use of a stochastic model for the accelerations of a runner. We have checked that the runner's acceleration are stationary process during all the trials: quite remarkably there is no deterministic drift, nor stochastic drift within any trial. Moreover, we have identified that the correlation function ρ is very similar for every runner and every intensity. This underlying and common structure is simple and well-described by an $ARMA(2,1)$. This implies that the constant acceleration ability has to be understood as a long-term trend, that is achieved through constant stochastic corrections of the short-term accelerations. Additionally, this control of the accelerations is maintained until exhaustion.

The autocovariance functions show that the accelerations between times t and $t+1$ are uncorrelated, whereas the correlations between times t and $t+2$ and $t+3$ are significantly negative. This suggests a control mechanism that have a 1 second delay, followed by a 2 seconds period for small corrections towards the mean $\boldsymbol{A}$. Higher order correlations are then null. The mechanism is a mean reverting process but is more elaborated than a simple mean-reverting $AR(1)$ process such that $A_{t+1} = \phi A_t + (1-\phi)\mathbf{A} + e_t$. In this latter case, the autocorrelation functions is geometric $\rho(h) = \phi^h > 0$ and is not able to reproduce this specific 3 seconds pattern identified in section 3.1.3. While in a first order process, the correction is directly proportional to the instantaneous difference $(A_t - \mathbf{A})$, the runner's feedback seems to use a buffer that is compared to an expected objective to be delineated.

A possible direction to investigate is the remarkable deterministic relationship between run distance and time $D_t = V_0 t + \boldsymbol{A}\frac{t(t+1)}{2} + X_t$, as plotted in figure 3. Paradoxically, $(X_t)_{t\geq 0}$ is a unit-root process which implies that the variance $V(X_t)$ should diverge as its definition $X_t = \sum_{i=1}^{t} (t+1-i)\, Z_i$ suggests (indeed it is a random walk). Instead, the variance $V(X_t)$ is significantly reduced thanks to the correlation structure of the variations $(Z_t)_{t\geq 0}$ as we have

$$V(X_t) = \sigma_Z^2 \left\{ \sum_{i=1}^{t} (t+1-i)^2 + 2 \sum_{i<j} (t+1-i)(t+1-j)\, \rho_Z(i-j, \boldsymbol{\theta}, \boldsymbol{\phi}) \right\}.$$

If we consider that $\rho_Z(h) = \rho_Z(h, \boldsymbol{\theta}, \boldsymbol{\phi})$ vanish for all h but $h = 2, 3$, we have

$$\begin{aligned} \frac{V(X_t)}{\sigma_Z^2} &= \sum_{i=1}^{t} (t+1-i)^2 + 2\,(t+1-i)\,\{(t+1-i+2)\,\rho_Z(2) + (t+1-i+3)\,\rho_Z(3)\} \\ &= \sum_{i=1}^{t} (t+1-i)\,(t+3-i)\,(1 + 2\rho_Z(2) + 2\rho_Z(3)) + 2\,(\rho_Z(3) - 1) \sum_{i=1}^{t} (t+1-i) \end{aligned}$$

The variance function $V(X_t)$ can be made quite small on a time range $[0, T]$ for appropriate choice of correlations $\rho_Z(2)$, $\rho_Z(3)$: the leading term $1 + 2\,(\rho_Z(2) + \rho_Z(3))$ nearly vanishes for $\rho_Z(2), \rho_Z(3)$ between -0.2 and -0.3. This suggests that the run distance could be part of a feedback loop for controlling the acceleration based on expected time laps, in the same way as the influence of the remaining distance in 800m and 1500m races has already been pointed out (Billat et al. (2009)). Obviously, such strategies remain hard to characterize, and the mechanisms used to avoid the divergence of the speed during these self-pace trials still need to be estimated.

We remark that the speed data $\left(\hat{V}_t\right)_{t=1\ldots T}$ still can be analysed directly, within our framework of a (stationary) ARMA model. Nevertheless, the stochastic structure is less easy to characterise, or at least, the common features are less easy to extract. Indeed, the hyperparameters p, q, as the estimates $\hat{\boldsymbol{\theta}}^{i,j}$ and $\hat{\boldsymbol{\phi}}^{i,j}$ may vary between trials and runners, and the features of the autocovariance functions are faded. This indicates that the standard speed data are less informative about the structure of the movement and strategy of the runners, because they are observed with some noise, and because the speed signal is an integrated acceleration signal, which causes fading of the information provided by the acceleration. As the use and analysis of real acceleration data in running is relatively new, this might explain why such a domain has been poorly addressed until now.

Furthermore, these freely chosen accelerations also corresponded to the imposed acceleration values frequently used in treadmill ramp protocols for determining VO2max (Myers and Bellin (2000); Porszasz et al. (2003)). In ramp protocols, the work rate is ramped up as a continuous increase and then a continuous acceleration. Given that the linearity of the oxygen uptake response is a major discriminating cardiovascular feature for assessing exercise intolerance, it is important to be sure that the work rate profile is linear and then the acceleration is constant. That is, why the tests are currently performed on a treadmill. Ramp testing on a treadmill was first described in 1991 by Myers et al. Even though manufacturers have developed a range of technologies for enabling ramp tests (e.g. controlled cycle ergometer), some subjects have difficulty walking and running on a treadmill and then reaching their maximum VO2 and speed at VO2max. It has been argued that the treadmill useful induces a higher maximum metabolic rate (compared with a cycle ergometer) and uses a mode of exercise that more closely approximates some activities of daily living (Balke and Ware (1959); Ellestad (1996); Froelicher et al. (2000)). In a much easier protocol, the present study shows that male and female middle-aged, recreational runners were able to self-monitor acceleration and thus reproduced an outdoor ramp protocol. Indeed, the present results showed that it is possible to apply a self-paced, ramp-like running protocol on the track. Regardless of the acceleration level (soft, medium or high), the SAT protocol uses a continuous change in speed and brings the subjects to exhaustion in approximately 3 to 12 minutes; this meets the criteria for clinical exercise testing issues by the relevant international organizations (of Sports Medicine et al. (2013); Society et al. (2003); Casaburi et al. (1997); Myers et al. (1992); Gibbons et al. (1997); Will and Walter (1999)). Given that, it has been proved that the environmental setting influences physiological, perceptual and affective responses during exercise at a self-selected pace (Dasilva et al. (2011)), we did not measure oxygen uptake because of the mask wearing which could have hamper the runners, the present results at least indicate that the maximum heart rate was achieved at all three acceleration levels and that the plateau at the maximal heart rate was only significantly different between the low and high acceleration trials ($p = 0.004$).

5 Conclusion

We show that (recreational) runners can precisely regulate their acceleration (regardless of its intensity) in a run leading to exhaustion in 3 to 14 minutes. This paper shows that the acceleration is stochastic, and constant acceleration is achieved by short-term, delayed, local corrections of the instantaneous acceleration. As a consequence, the speed and distance run are driven by a deterministic constant acceleration trend. This shows that Humans are able to develop the feeling of their own body acceleration. Question remains of the mechanism of this acceleration control. Neurophysiologists have demonstrated that Human brain imposes in a top-down fashion its rules of interpretation of sensory data. It transforms the perceived world according to the rules of symmetry, stability and kinematic laws derived from principles of maximum smoothness (Berthoz (2008)). It has been shown that Humans have the perception of distance (Mossio et al. (2008)), hence a possibility to explore is that Humans have also the feeling of run distance, as it is now assessed that the vestibular system plays a fundamental role in spatial orientation and is also involved in the memory of travelled paths (Israel and Berthoz (1989); Berthoz et al. (1995)).

The mathematical model proposed to assess these claims is interesting on its own. It is a simple stochastic model of the acceleration, that is remarkably stable across the different intensities and the runners. Our model is a stationary ARMA process for acceleration, whose mean is controlled by the runner. An ongoing work is to validate and generalize such a model from our sample to a wider population, and also in the case where more elaborate acceleration patterns are to be reached. This work is ongoing in runners of different levels, for comparing this control process according to the runner's experiences. This preliminary work might give the possibility for a runner to control his acceleration when running, which is promising for the exercise and energy resources self-management in the context of exercise health and performance. Such future works might help in identifying the mechanism of controls used by a runner during a trial or a race. The use and analysis of acceleration data from reliable accelerometer seems crucial for this step.

Indeed, our analysis of acceleration, speed and distance data indicates that we should focus on acceleration and distance data, as they are more insightful and precise than speed, and becomes easier to measure thanks to the important development of accelerometers.

Supporting information

Supplementary Information 1 Statistical Analysis of all runners. We gather the description and statistical analysis of all the runners, for all trial intensities.

References

Abbiss, C. R. and Laursen, P. B. (2008). Describing and understanding pacing strategies during athletic competition. *Sports Medicine*, 38(3):239–252.

Ansley, L., Noakes, T., Robson-Ansley, P., and St Clair Gibson, A. (2004). Anticipatory pacing strategies during supra-maximal exercise lasting more than 30 s. *Medicine & Science in Sports & Exercise*, 36(2):309–314.

Ariyoshi, M., Yamaji, K., and Shephard, R. (1979). Influence of running pace upon performance: effects upon treadmill endurance time and oxygen cost. *European journal of applied physiology and occupational physiology*, 41(2):83–91.

Balke, B. and Ware, R. W. (1959). An experimental study of physical fitness of air force personnel. *United States Armed Forces Medical Journal*, 10(6):675–688.

Bencsik, L. and Zelei, A. (2017). Effects of human running cadence and experimental validation of the bouncing ball model. *Mechanical Systems and Signal Processing*, 89:78–87.

Berthoin, S., Baquet, G., Rabita, J., Blondel, N., et al. (1999). Validity of the universite de montreal track test to assess the velocity associated with peak oxygen uptake for adolescents. *Journal of sports medicine and physical fitness*, 39(2):107.

Berthoz, A. (2008). *Neurobiology of" Umwelt": how living beings perceive the world.* Springer Science & Business Media.

Berthoz, A., Israël, I., Georges-François, P., Grasso, R., and Tsuzuku, T. (1995). Spatial memory of body linear displacement: what is being stored? *Science*, 269(5220):95.

Billat, L. V. and Koralsztein, J. P. (1996). Significance of the velocity at vo2max and time to exhaustion at this velocity. *Sports Medicine*, 22(2):90–108.

Billat, V., Hamard, L., Koralsztein, J. P., and Morton, R. H. (2009). Differential modeling of anaerobic and aerobic metabolism in the 800-m and 1,500-m run. *Journal of Applied Physiology*, 107(2):478–487.

Billat, V. L., Lepretre, P.-M., Heugas, A.-M., and Koralsztein, J. P. (2004). Energetics of middle-distance running performances in male and female junior using track measurements. *The Japanese journal of physiology*, 54(2):125–135.

Billat, V. L., Slawinski, J., Danel, M., and Koralsztein, J. P. (2001). Effect of free versus constant pace on performance and oxygen kinetics in running. *Medicine & Science in Sports & Exercise*, 33(12):2082–2088.

Blickhan, R. (1989). The spring-mass model for running and hopping. *Journal of biomechanics*, 22(11-12):1217–1227.

Bramble, D. M. and Lieberman, D. E. (2004). Endurance running and the evolution of homo. *Nature*, 432(7015):345–352.

Casaburi, R., Prefaut, C., and Cotes, J. (1997). Equipment, measurements and quality control in clinical exercise testing. *Monograph*, 6:72–87.

Crouter, S., Foster, C., Esten, P., Brice, G., and Porcari, J. P. (2001). Comparison of incremental treadmill exercise and free range running. *Medicine and science in sports and exercise*, 33(4):644–647.

Dasilva, S. G., Guidetti, L., Buzzachera, C. F., Elsangedy, H. M., Krinski, K., De Campos, W., Goss, F. L., and Baldari, C. (2011). Psychophysiological responses to self-paced treadmill and overground exercise. *Medicine & Science in Sports & Exercise*, 43(6):1114–1124.

De Koning, J. J., Foster, C., Bakkum, A., Kloppenburg, S., Thiel, C., Joseph, T., Cohen, J., and Porcari, J. P. (2011). Regulation of pacing strategy during athletic competition. *PloS one*, 6(1):e15863.

Ellestad, M. (1996). Cardiovascular and pulmonary responses to exercise. *Stress testing: principles and practice. 4th ed. Philadelphia, PA: FA Davis Company*, pages 11–41.

Farley, C., Blickhan, R., Saito, J., and Taylor, C. (1991). Hopping frequency in humans: a test of how springs set stride frequency in bouncing gaits. *Journal of Applied Physiology*, 71(6):2127–2132.

Flash, T. and Hogan, N. (1985). The coordination of arm movements: an experimentally confirmed mathematical model. *Journal of neuroscience*, 5(7):1688–1703.

Foster, C., Green, M. A., Snyder, A. C., and Thompson, N. N. (1993). Physiological responses during simulated competition. *Medicine and science in sports and exercise*, 25(7):877–882.

Foster, C., Hettinga, F., Lampen, J., Dodge, C., Bobbert, M., Porcari, J., et al. (2004). Effect of competitive distance on energy expenditure during simulated competition. *International journal of sports medicine*, 25(03):198–204.

Foster, C., Schrager, M., Snyder, A. C., and Thompson, N. N. (1994). Pacing strategy and athletic performance. *Sports Medicine*, 17(2):77–85.

Froelicher, V. F., Myers, J., Follansbee, W., and Labovitz, A. (2000). Exercise and the heart. *Chest*, 118(1).

Gibbons, R. J., Balady, G. J., Beasley, J. W., Bricker, J. T., Duvernoy, W. F., Froelicher, V. F., Mark, D. B., Marwick, T. H., McCallister, B. D., Thompson, P. D., et al. (1997). Acc/aha guidelines for exercise testing: a report of the american college of cardiology/american heart association task force on practice guidelines (committee on exercise testing). *Journal of the American College of Cardiology*, 30(1):260–311.

Hamilton, J. D. (1994). *Time series analysis*, volume 2. Princeton university press Princeton.

Hreljac, A. (2000). Stride smoothness evaluation of runners and other athletes. *Gait & posture*, 11(3):199–206.

Hreljac, A. and Martin, P. E. (1993). The relationship between smoothness and economy during walking. *Biological Cybernetics*, 69(3):213–218.

Hunter, J. P., Marshall, R. N., and McNair, P. J. (2005). Relationships between ground reaction force impulse and kinematics of sprint-running acceleration. *Journal of applied biomechanics*, 21(1):31–43.

Israel, I. and Berthoz, A. (1989). Contribution of the otoliths to the calculation of linear displacement. *Journal of neurophysiology*, 62(1):247–263.

Lambert, M. I., Dugas, J. P., Kirkman, M. C., Mokone, G. G., and Waldeck, M. R. (2004). Changes in running speeds in a 100 km ultra-marathon race. *Journal of sports science & medicine*, 3(3):167.

Larsson, P. (2003). Global positioning system and sport-specific testing. *Sports Medicine*, 33(15):1093–1101.

Larsson, P. and Henriksson-Larsén, K. (2005). Combined metabolic gas analyser and dgps analysis of performance in cross-country skiing. *Journal of sports sciences*, 23(8):861–870.

McMahon, T. A. and Cheng, G. C. (1990). The mechanics of running: how does stiffness couple with speed? *Journal of biomechanics*, 23:65–78.

Mossio, M., Vidal, M., and Berthoz, A. (2008). Traveled distances: New insights into the role of optic flow. *Vision research*, 48(2):289–303.

Myers, J. and Bellin, D. (2000). Ramp exercise protocols for clinical and cardiopulmonary exercise testing. *Sports Medicine*, 30(1):23–29.

Myers, J., Buchanan, N., Smith, D., Neutel, J., Bowes, E., Walsh, D., and Froelicher, V. F. (1992). Individualized ramp treadmill: observations on a new protocol. *Chest*, 101(5):236S–241S.

of Sports Medicine, A. C. et al. (2013). *ACSM's guidelines for exercise testing and prescription*. Lippincott Williams & Wilkins.

Poole, D. C., Wilkerson, D. P., and Jones, A. M. (2008). Validity of criteria for establishing maximal o2 uptake during ramp exercise tests. *European journal of applied physiology*, 102(4):403–410.

Porszasz, J., Casaburi, R., Somfay, A., Woodhouse, L. J., and Whipp, B. J. (2003). A treadmill ramp protocol using simultaneous changes in speed and grade. *Medicine &*

Science in Sports & Exercise, 35(9):1596–1603.

Sandals, L. E., Wood, D., Draper, S. B., and James, D. (2006). Influence of pacing strategy on oxygen uptake during treadmill middle-distance running. *International journal of sports medicine*, 27(01):37–42.

Society, A. T. et al. (2003). Ats/accp statement on cardiopulmonary exercise testing. *American journal of respiratory and critical care medicine*, 167(2):211.

Tucker, R., Lambert, M. I., and Noakes, T. D. (2006). An analysis of pacing strategies during men's world-record performances in track athletics. *International journal of sports physiology and performance*, 1(3):233–245.

Tucker, R. and Noakes, T. D. (2009). The physiological regulation of pacing strategy during exercise: a critical review. *British Journal of Sports Medicine*, 43(6):e1–e1.

Uger, L. and Boucher, R. (1980). An indirect continuous running multistage field test: the universite de montreal track test. *Can. J. Appl. Sport. Sci*, 5:77–84.

Will, P. M. and Walter, J. D. (1999). Exercise testing: improving performance with a ramped bruce protocol. *American heart journal*, 138(6):1033–1037.

Zamparo, P., Perini, R., Peano, C., and di Prampero, P. (2001). The self selected speed of running in recreational long distance runners. *International journal of sports medicine*, 22(08):598–604.